THE EXPERIMENTAL INVESTIGATION OF THE SPATIAL VORTEX PATTERNS OF SOME SLENDER BODIES AT HIGH ANGLE OF ATTACK IN LOW SPEED TUNNEL

Wu Genxing, Wang Tzehsing and Tian Shizhong
Nanjing Aeronautical Institute
Nanjing, China

Abstract

The method of the flourescent mini-tuft has been used to investigate the changes of the spatial vortices with the angle of attack on lee side of some slender bodies in low speed tunnel without sideslip. Four models of slender bodies with different section have been used. Top view as well as side view of the vortex have been acquired. The axial velocities of the vortex by the hot wire anemometer and the circulation of the vortex by the method of the flourescent mini-tuft along the track of vortex are measured. Both have been given for the symmetric and asymmetric vortex pattern on the sharp ogive body of revolution. This investigation clearly shows the relations of the asymmetric side force to the asymmetric vortices. Also, the model of the asymmetric vortices and the interference between the vortices are realized to some extent. The effects of the disturbance caused by a small protrustion at the fore part of the slender body on the position of vortex are also investigated.

Introduction

It is necessary for modern aircraft and missiles to fly at large angles of attack in order to obtain high manoeuvrability. With increasing angle of attack, the vortex patterns on the lee-side of slender bodies become asymmetric even without sideslip. The asymmetric vortices produce an unwilling large side force and yawing moment. The mechanism of the asymmetric vortex pattern is not clearly understood to assure prediction yet. In the past, most of the researchs of asymmetric vortex have been restricted to the force and moment measurements in the wind tunnels to study the effect of the geometric parameter of the body on the side force.[1][2] Nevertheless it is lack that the spatial vortex pattern, the interference between vortices, the axial velocity of the vortex core centre and the circulation of the vortex along the vortex tracks are investigated. Some researchers have only measured the pattern and circulation of vortex at a few sections.[3][4][5] While others have acquired the side view of vortex track by schlierengraph.[6] The top view of the vortex track have not been shown yet.

The objective of present study is to measure the change of spatial vortex tracks with angles of attack on lee side of some slender bodies in low speed tunnel without sideslip. The method of the flourescent mini-tuft is used so that the vortex pattern can be acquired in detail and more completely. The top view as well as side view of the vortex tracks have been shown. Four different slender bodies are studied in order to realize the effect of the geometry of the body on the vortex pattern. The axial velocity of the vortex core centre measured with the hot wire anemometer and the circulation of the vortex measured by the method of the flourescent mini-tuft along the vortex tracks have been given for the symmetric and asymmetric vortex pattern on the sharp ogive body of revolution so that the character of the spatial vortex can be clearly understood. The effects of the distur-

bance caused by a small protrusion at the fore part of the slender body on the vortex tracks are also investigated.

Description of the model and experiment equipment

The vortex trails was measured in a 0.75x0.75 meter low speed wind tunnel at a velocity of wind of 30 m/s. The Reynolds number was about 1.2×10^5 based on the diameter of the cylindric part of slender bodies. The angle of attack of the model was from 10° to 60°. The axical velocity of vortex core centre and the circulation of the vortex were measured in the 1.5x1.5 meter low speed wind tunnel. The size of the large model was twice as long as the small model. The test Reynolds number was about 1.6×10^5.

Figure 1. shows the shape of four slender bodies of different section shape. The nose fineness ratio is 3.5 and the afterbody fineness is also 3.5. The afterbody is of cylindric shape. The difference among these four models are shown in Figure 1. in detail.

The method of the flourescent mini-tuft is used to measured the tracks and the circulation of the spatial vortex.(7) The flourescent mini-tuft is made of nylon filament. It's diameter is about 0.02 mm. It is treated in special material in order to decrease the static electric effect. When it is set in the vortex flow, the rotary speed of the mini-tuft was measured by nitrogen molecule Laser, so the circulation of the vortex can be calculated. The spatial vortex track was recorded by the camera. The coordinate of vortex track and the circulation of vortex was dimensionless. The length of model, L and the maximum circulation, Γ_{MAX} along the vortex track are used as reference.

Results and Discussion

A. The change of the vortex track on the sharp revolution body with the angle of attack, α without sideslip

The change of the side force with α without sideslip has been given in reference (1, 2) for sharp and blunted body of revolution. It has been shown that at the angle of attack more than about 30° the side force is generated for the sharp revolution body. It increased continually with increasind α and was maximum at about $\alpha=45^\circ$, then it decreased with increasing α. The angle of attack at which the side force is generated for the blunted revolution body is large than that for the sharp revolution body. The maximum side force for the blunted revolution body is less than that for the sharp revolution body. The change of the vortex tracks with α can be divided into the following stages:

(1) Partial symmetric vortex pattern ($\alpha<10^\circ$). In this stage there is attached flow in the front of the body, however there are two symmetric vortices in the rear of the body (see Fig. 2). The point where the symmetric vortex originates move from the base to the apex of the body with increasing α.

(2) Whole symmetric vortex pattern ($\alpha=12^\circ$-30°). There are two symmetric vortices originated from the apex of the body and extended to the base of the body on leeside. The vortex tracks are above the cylinder and nearly parallel to the axis of the body as shown in Fig.3. It can also be shown that both the axail velocities of the vortex cores and the vortex circulation of the two symmetric vortices are equal and increases along the vortex track as shown in Figure 4. It can be illustrated that separation vortex around the circular cylinder in the two-dimensional case are fed into the spatial vortex on the lee side of the body. The flow around the slender body is similar to the two-dimensional flow around a circular cylinder. Besides a pair of main vortices, there is a pair of second

vortices with rotation direction same as that of the main vortices and its position is near the separation line. There is still a pair of secondary vortex induced by the main vortex as shown in the test of the oil flow. Its rotation direction is contra to the main vortex. Its core is smaller than the main vortex. The position of the main and the second vortex lift up continuly with increasing α as shown in Figure (3) (5). The second and secondary vortex are usually negligible.

(3) Two asymmetric vortices pattern ($\alpha = 30^\circ$-47°). As $\alpha > 30^\circ$, the circulation and the position of the symmetric vortex at the base of the body would develop to some state, similar to the flow pattern of a cylinder starting from rest[8] the two main vortices begin to become asymmetric from the base of the body. One of them is lower, while the other is higher and slightly turnning up near the base of the body. Because of the inductive effect between each other, the lower vortex is near to the symmetric plane of the body, while the higher one bends further away. (see Figure 5.). Therefore the side force and moment are created obviously. With increasing α, the asymmetric phenomenon becomes violent and moves forwards. The rear of the higher vortex gradually begin to turn up parallel to the free stream. With the turnning up of the main vortices, the second vortices lift up.

The change of axial velocity of the vortex cores and the circulation of the main vortex at $\alpha = 45^\circ$ are given in Figure 6. It can be shown that when the vortices turn up, the axical velocity and the circulation of the vortex begin to decrease for asymmetric state. It shows that the vortex gradually begins to shed from the body and becomes the free vortex. The separated vortex around the circular cylinder no longer fed into the turnning up vortex, while it fed into the second vortex. The second vortex circulation is increased. It gradually becomes the second main vortex whose effect can not be negleeted. This is similar to vortex shedding process behind two-dimensional circular cylinder. Comparison of the axial velocity and the circulation of two vortices indicates that if the vortex tracks are symmetric, the axial velocity and the circulation are equal approximately on the forebody ($x/L < 0.5$). The vortex tracks are asymmetric obviously for $x/L > 0.5$. Both the axial velocity and the circulation of the lower vortex are obviously larger than that of the higher one. The inductive effect of the lower vortex on the body is more strong than that of the higher one.

The maximum value of the circulation at $\alpha = 45^\circ$ is twice as large as at $\alpha = 22.5^\circ$. It can be shown that the circulation of the vortex increases with α.

(4) Three asymmetric vortex pattern ($\alpha = 47^\circ$-55°). After the second vortex has become the second main vortex, the asymmetric two vortex pattern changes into asymmetric three vortex pattern as shown in Figure 7. Under the inductive effect of the main vortex of other side, the second main vortex always turns to the symmetric plane of the body. The main vortex of other side deflects apart from the symmetric plane of the body. Therefore the asymmetric side force does not increase and begins to decrease. The maximum side force occures at this stage at which two main vortex deflect most severely and the second vortex does not become the second main vortex. The main vortex of other side begins to diverge at this stage.

(5) Asymmetric multiple vortex pattern ($\alpha > 55^\circ$). After the second main vortex has begun to turn up and become the free vortex, as mentioned above, a third main vortex will occur under the second main vortex. The vortex breakdown will appear in the rear of the main vortex of the other side, as shown in Fig. 8.

(6) Asymmetric vortex with the wake region ($\alpha > 60^\circ$). When the angle of attack is very large, the point at which the vortex begins to turn up and deflect moves forwards from the back to the apex of the body. At this time, the vortex breakdown can appear in the rear of the high main vortex. Therefore the wake region begins to appear on the lee side in the rear of the body. When $\alpha > 70^\circ$, except in the region of the head of the body, the rest of the body is wake region as shown in Fig.9. The side force disappears.

B. The change of the vortex track with α on the blunted revolution body and the sharp slender body with the horizontal or perpendicular elliptical section

The process of change of the vortex track of these bodies is similar to that of the sharp revolution body. The angle of attack at which the various vortex pattern appears is different, as listed in table 1.

VORTEX PATTERN	ANGLE OF ATTACK (deg.)			
	model 1.	model 2	model 3	model 4
PARTIAL SYMMETRIC	<12	<22	<10	<16
WHOLE SYMMETRIC	12-30	22-38	10-30	16-20
TWO ASYMMETRIC	30-47	38-48	30-45	20-25
THREE ASYMMETRIC	47-55	48-57	>45	>25

TABLE 1. THE ANGLE OF ATTACK FOR VARIOUS VORTEX PATTERN

The particular characters are:

(1) For blunted revolution body, owing to the effect of flow around the blunted head, the change of the partial symmetric vortex pattern into the whole symmetric vortex pattern is delayed, the angles of attack at which the two and three asymmetric vortex patterns occur are also delayed. Comparison of Figure 5 and 10 indicates that the vortex deflection generated on the blunted revolution body is more moderate than on the sharp revolution body. Therefore the asymmetric side force on the blunted revolution body is less than that on the sharp revolution body.

(2) For sharp slender body with horizontal elliptical section, only the three asymmetric vortex pattern appears. When $\alpha > 50^\circ$, the vortex breakdown appears in the rear of the main vortex of the other side as shown in Figure 11. Therefore before the third vortex takes place, the rear of the body becomes the wake region.

As increasing α, the high and the low vortex change atternately. For example, when $\alpha = 30^\circ$ the right vortex is higher than the left vortex. While $\alpha = 40^\circ$ they are reversed.

(3) For the sharp slender body with perpendicular elliptical section, once the whole symmetric vortex pattern is formed, the asymmetric two vortex pattern will appear soon. Like the two-dimensional flow around the circular cylinder the vortices will alternately shed from both sides of the body. The vortex pattern is similar to Kármán street pattern as shown in Figure 12. As $\alpha > 30^\circ$ the divergence and the breakdown of the vortex which appear for three bodies as mentioned above can not be observed in this case.

C. The effects of disturbance on the spatial vortex track

A small protrusion whose height and area are about 1/50 of the diameter and 0.5% of the section area of the model correspondently was set at the fore part of the model of the sharp revolution body in order to study the effect of disturbance on the spatial vortex track. Because of the effect of the axial flow, the vortex generated by the disturbance at the head moves along the freestream approximately. Therefore the disturbance only affect its down stream track. It is found that for symmetric vortex pattern the down stream

local track can move down due to the disturbance, however the vortex track near the rear of the body is hardly affacted as shown in Figure 13.

As for asymmetric vortex pattern, if the disturbance was set at the side of the higher vortex, the disturbance affects its whole down stream track strongly; while the effect of the disturbance on the lower vortex of the other side is smaller as shown in Figure 14. Comparison of Figure 5 and 14 indicates that the disturbance can move down the higher vortex track of the down stream and its position can be lower than the lower vortex of other side. Owing to the inductive effect of vortices between each other, the higher vortex always deflects apart from the symmetric plane of the body. It can be illustrated that the symmetric vortex pattern is more stable, it seems to be able to absorb the disturbance. However, the asymmetric vortex pattern seems not so stable. Once there is a disturbance, it can change its track immediately. The problems of the vortex stabilization have still to be study further.

Conclusions

1. The change of the vortex tracks with the angle of attack is almost the same. The development of the vortex track follows the following process; partial symmetric vortex pattern (for sharp revolution body $\alpha < 12°$) ——→whole symmetric vortex pattern ($\alpha < 30°$) ——→asymmetric two vortex pattern ($\alpha < 47°$), the asymmetric side force is maximum in this range.——→asymmetric three vortex pattern ($\alpha < 55°$), the side force begins to decrease——→asymmetric multiple vortex pattern ($\alpha < 60°$)——→asymmetric vortex plus the wake pattern ($\alpha > 60°$).

2. Besides some general characters of the vortices, there are some particulars for slender bodies of different shape. For example, the angle of attack at which the asymmetric vortex pattern occurs is delayed and the vortex deflection is more moderate for the blunted revolution body. However the asymmteric vortex pattern can appear more early and is similar to that of the Kármán's street for the sharp slender body with perpendicular elliptical section. For the sharp slender body with horizontal elliptical section only the three asymmetric vortex pattern is observed. The height of the right-left vortex track changes atternately.

3. The development of the vortices on the slender body with the increasing α is similar to the case of the two-dimensional circular cylinder starting from rest. Besides the right and left main vortices, there are a pair of second and secondary vortex whose rotary direction is the same as that of the main vortex and against respectively. When the main vortex have shed from the body and become the free vortex, the second vortex become a second main vortex.

4. After the second vortex have become the second main vortex, because of the inductive effect of each vortex, on the one hand the vortex track can be changed, on the other hand the vortex divergence and breakdown can appear in the rear of the lower main vortex. The asymmetric breakdown of the vortex can be noticed.

5. The down stream local track can move down due to the disturbance, however the vortex track near the rear of the body is almost not affected for symmetric vortex. As for asymmetric vortex, the disturbance can strongly affect the whole vortex track of down stream.The problems of the vortex stabilization have still to be study further.

References

1. Earl R. Keener, Gary T. chapman, Lee cohe, and Jamshid Taleghani, "Side forces

on a tangent ogive forebody with a fineness ratio of 3.5 at high angles of attack and Mach numbers from 0.1 to 0.7,", NASA TM X-3437. 1977.

2. Robert L. Kruse, Earl R. Keener, and Gary T. chapman, "Investigation of the Asymmetric Aerodynamic characteristics of cylindrical bodies of revolution with variations in Nose geometry and rotational orientation at angles of attack to 58° and Mach mumbers to 2," NASA TM 78533. 1979.

3. John E. Fidler, Richard G. Schwind, and Jack N. Niclsen "An Investigation of slender-body wake vortices," AIAA 15 th Aerospace Sciences meeting,volume 1. 1977.

4. William L. Oberkampf,F. Kevin Owen, T. P. Shivananda, "Experimental investigation of the asymmetric body vortex wake" AIAA Journal Vol.19, No. 8 , Aug. 1981.

5. Andrew B. Wardlan Jr., william J. Yanta, "Multistable vortex patterns on slender, circular bodies at high incidence," AIAA Journal Vol. 20, No.4, APR. 1982.

6. K. D. Thomson, D. F. Morrison, "The spacing, position and strength of vortices in the wake of slender cylindrical bodies at large incidence," Journal of Fluid Mechanics Vol.50, part 4,1971.

7. Wu Genxing, Wang Tzehsing, "The new method measuring the position and circulation of the spatial vortex in low speed tunnel," Proceeding of flow visualization and it's application meeting, Chinese Society of Mechanics, 1982.

8. A. E. Perry, M. S. Chong and T. T. Lim, "The vortex shedding process behind two dimensional bluff bodies" Journal Fluid Mech. Vol. 116, March 1982.

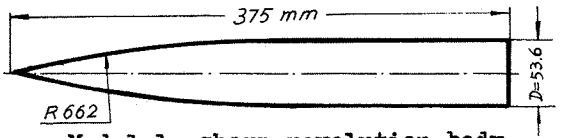

Model 1. sharp revolution body

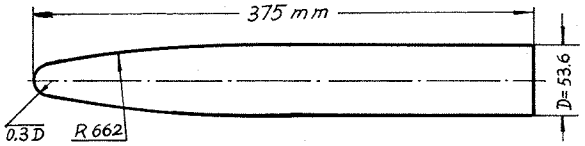

Model 2. blunted revolution body

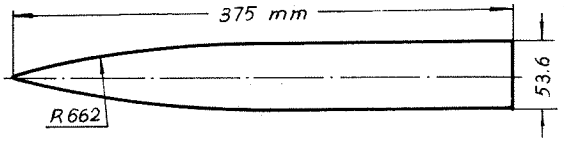

Model 3. sharp slender body with horizontal elliptical section

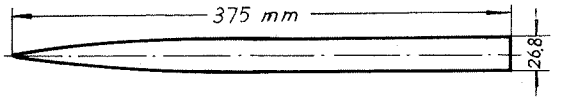

Model 4. sharp slender body with perpendicular elliptical section

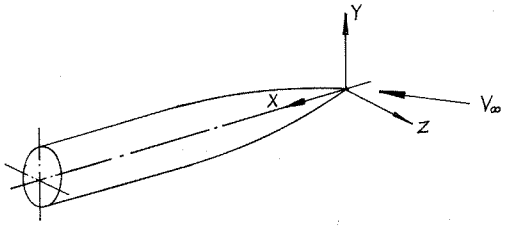

FIGURE 1. Model and coordinate

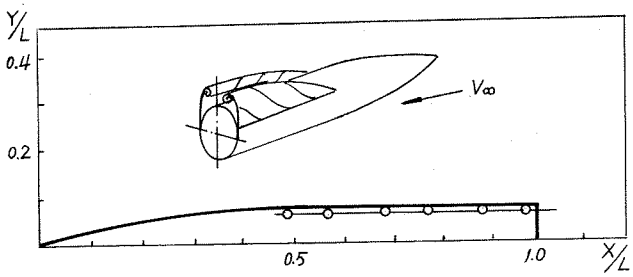

FIGURE 2. The vortex track for sharp revoltion body at $\alpha = 10^{\circ}$ (side view)

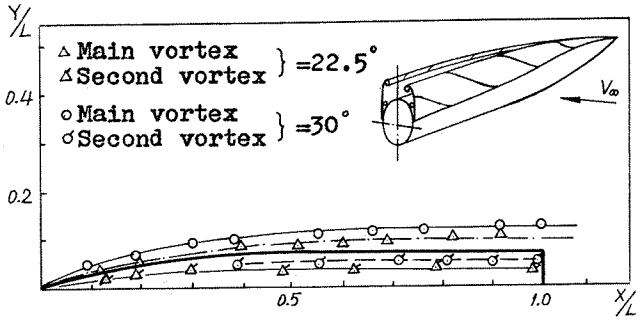

Fig. 3a side view

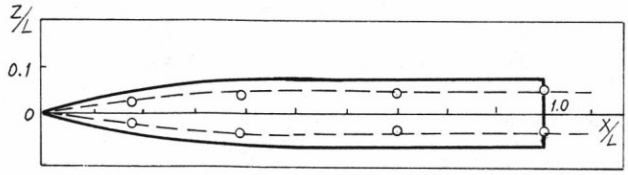

Fig. 3b top view

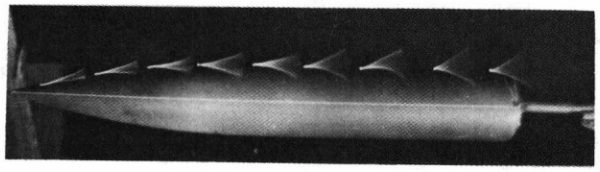

Fig. 3c photograph

FIGURE 3. The vortex track for sharp revolution body at α=22.5° and α=30°

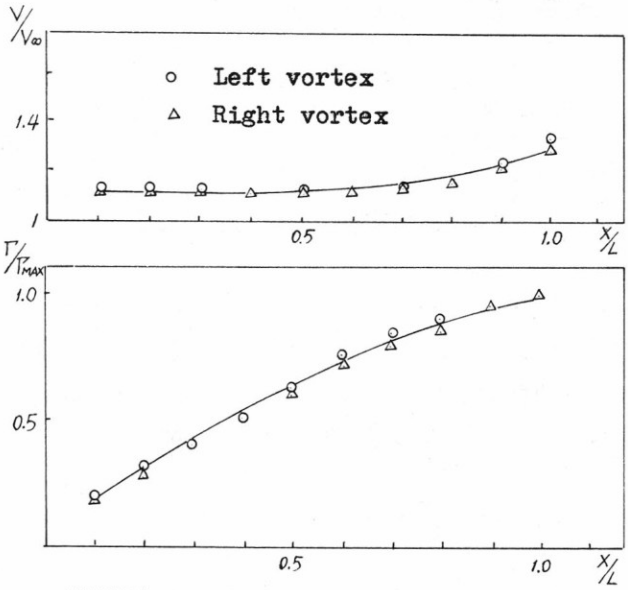

FIGURE 4. The axial velocity and the circulation of vortex along the vortex track for sharp revolution body at α =22.5°

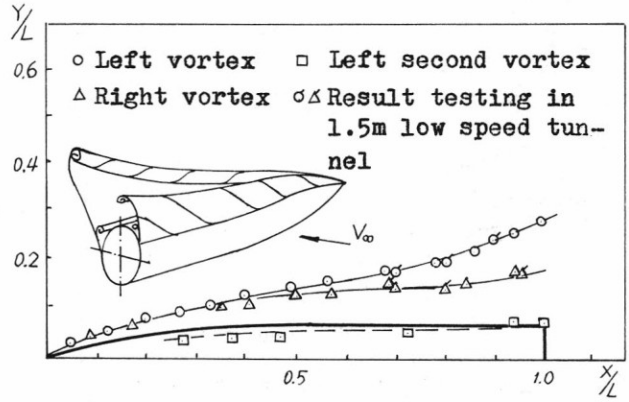

Fig. 5a side view

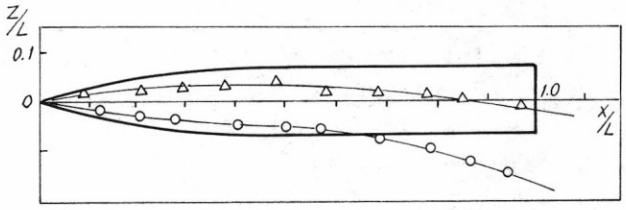

Fig. 5b top view

FIGURE 5. The vortex track for sharp revolution body at α = 45°

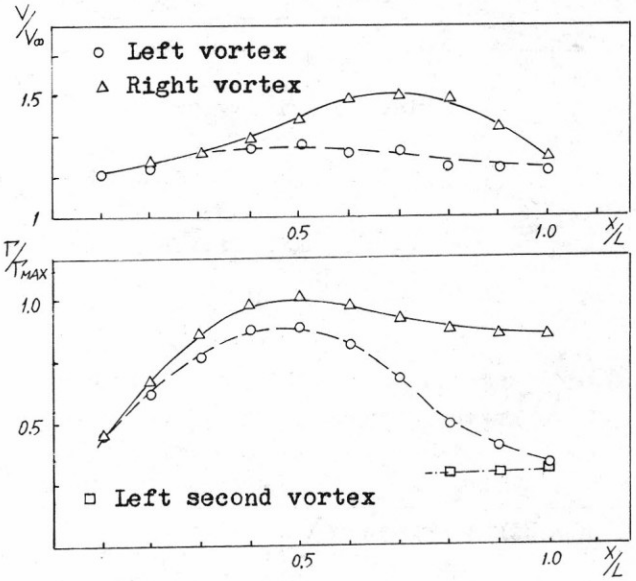

FIGURE 6. The axial velocity and the circulation of the vortex along the vortex track for sharp revolution body at α =45°

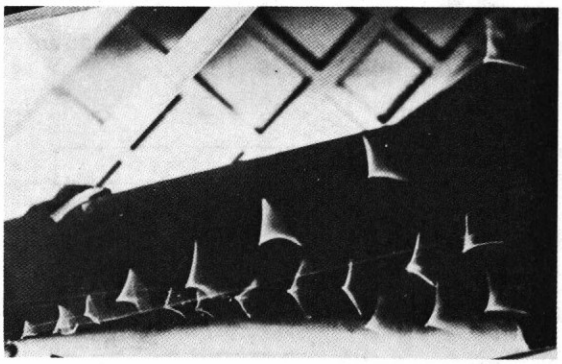

Fig. 7a photograph (side view)

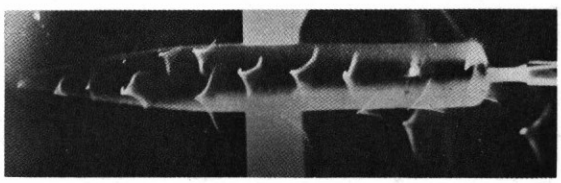

Fig. 7b photograph (top view)

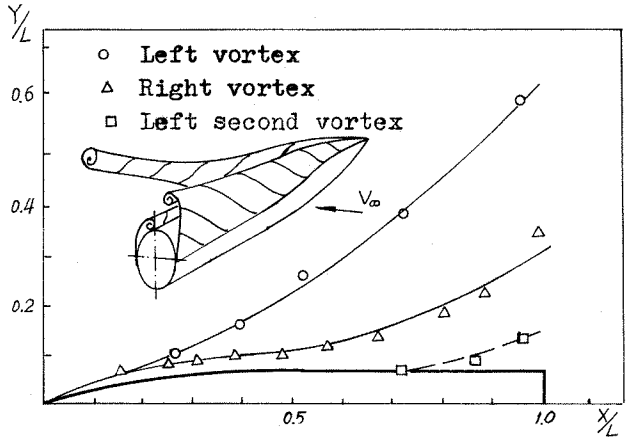

Fig. 7c side view

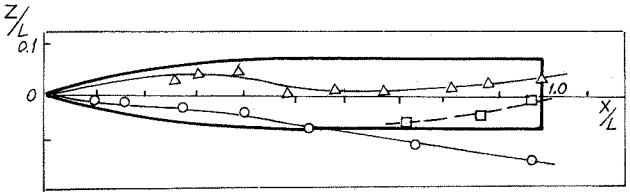

Fig. 7d top view

FIGURE 7. The vortex track for sharp revolution body at $\alpha = 50^\circ$

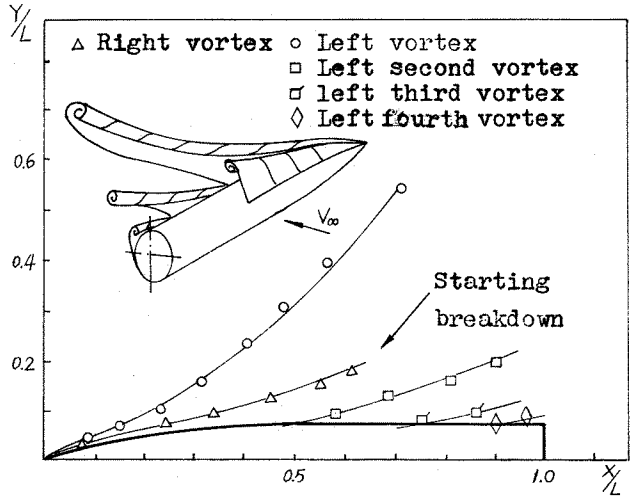

Fig. 8a side view

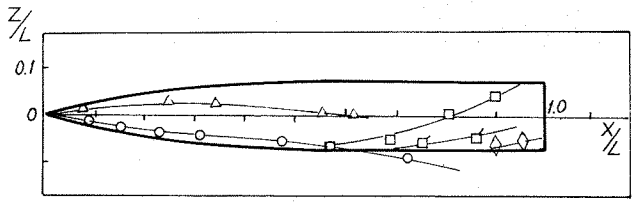

Fig. 8b top view

FIGURE 8. The vortex track for sharp revolution body at $\alpha = 55^\circ$

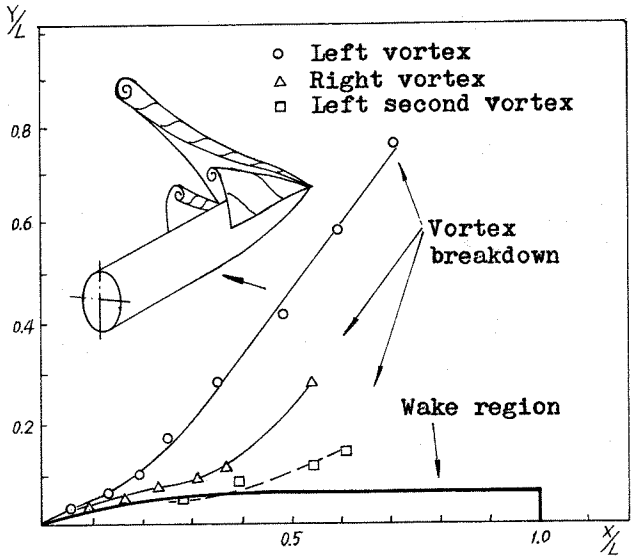

Fig. 9a side view

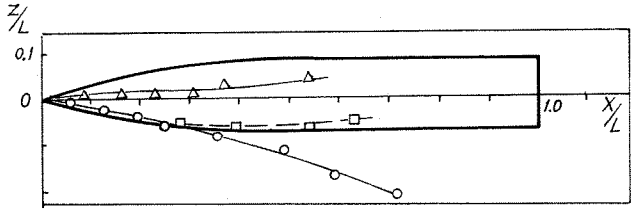

Fig. 9b top view

FIGURE 9. The vortex track for sharp revolution body at $\alpha = 60^\circ$

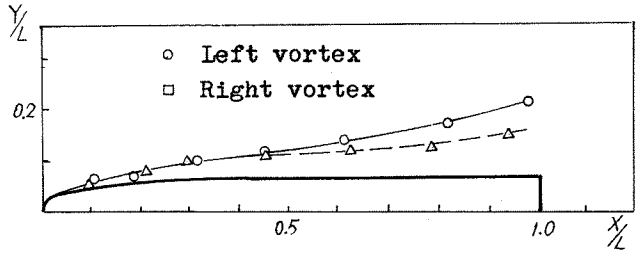

Fig. 10a side view

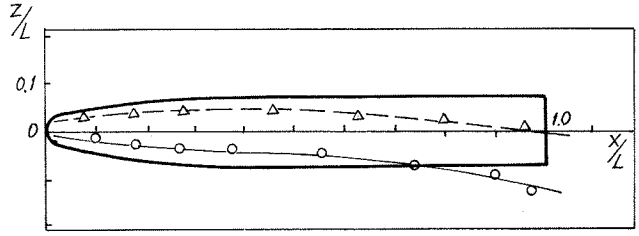

Fig. 10b top view

FIGURE 10. The vortex track for blunted revolution body at $\alpha = 45^\circ$

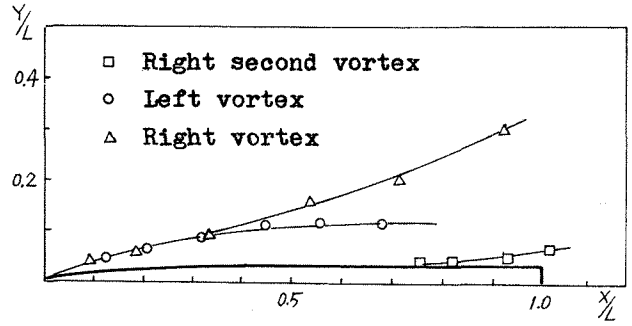

Fig. 11a side view

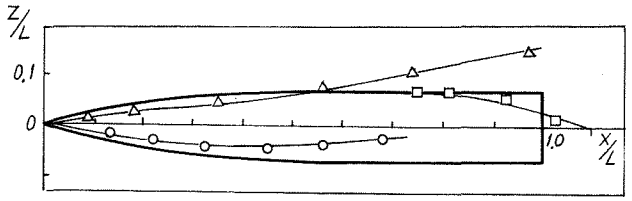

Fig. 11b top view

FIGURE 11. The vortex track for sharp slender body with horizontal elliptical section at $\alpha = 50^\circ$

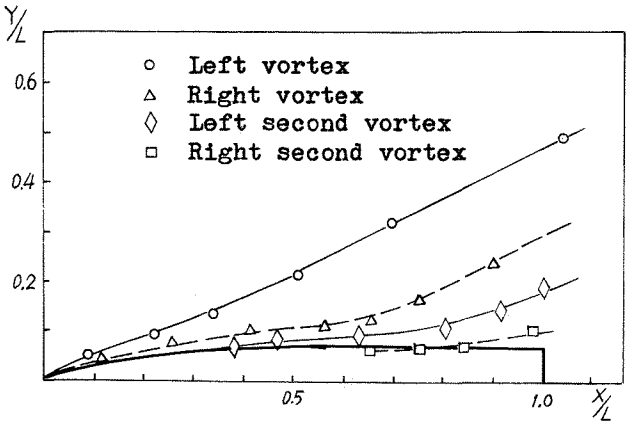

Fig. 12a side view

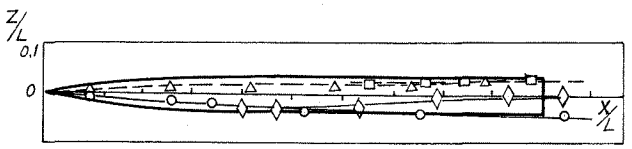

Fig. 12b top view

FIGURE 12. The vortex track for sharp slender body with perpendicular elliptical section at at $\alpha = 30^\circ$

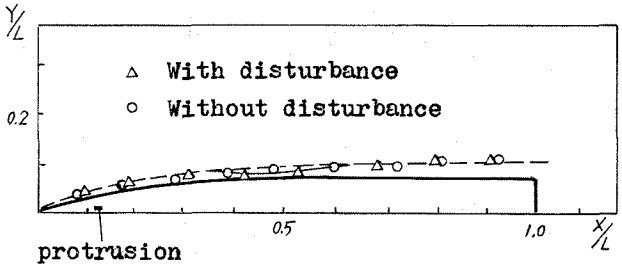

FIGURE 13. The effect of disturbance on the vortex track for sharp revolution body at $\alpha = 22.5^\circ$ (side view)

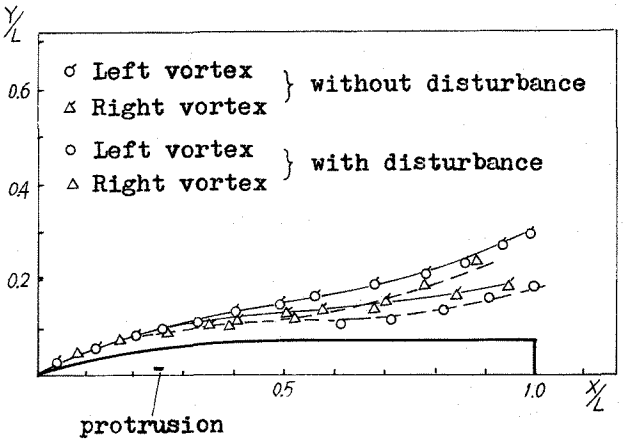

Fig. 14a side view

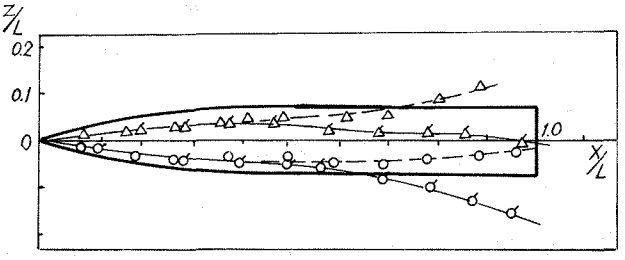

Fig. 14b top view

FIGURE 14. The effect of disturbance on the vortex track for sharp revolution body at $\alpha = 45^\circ$ (top view)